ELSEVIER

Journal of Alloys and Compounds 395 (2005) 240–246

Journal of ALLOYS AND COMPOUNDS

www.elsevier.com/locate/jallcom

Local bonding structure in mechanically activated TiH_2 and TiH_2 + graphite mixture

E.Z. Kurmaev[a], O. Morozova[b,*], T.I. Khomenko[b], Ch. Borchers[c], S.N. Nemnonov[a], Y. Harada[d], T. Tokushima[d], H. Osawa[e], T. Takeuchi[f], S. Shin[e]

[a] *Institute of Metal Physics, Russian Academy of Sciences-Ural Division, 620219 Yekaterinburg, Russia*
[b] *Semenov Institute of Chemical Physics, Russian Academy of Sciences, Kosygin st. 4, 119334 Moscow, Russia*
[c] *Institute of Materials Physics of Goettingen University, Tammannstr. 1, 37077 Goettingen, Germany*
[d] *Riken/Spring 8, Harima Institute, 1-1-1, Kouto, Mikazuki-Cho, Sayo-Gun, Hyogo, 679-5138, Japan*
[e] *Institute for Solid State Physics, University of Tokyo, 5-1-5 Kashiwanoha, Kashiwa-shi, Chiba 277-8581, Japan*
[f] *Tokyo University of Science, 1-3 Kagurazaka, Shinjuku, Tokyo 162-8601, Japan*

Received 26 April 2004; received in revised form 25 October 2004; accepted 8 November 2004
Available online 7 January 2005

Abstract

The local bonding structure of mechanically activated TiH_2 and TiH_2/graphite mixture is studied by means of temperature-programmed desorption (TPD), X-ray emission- and absorption-spectroscopy. Ball milling of TiH_2 in the presence of graphite results in a modification of the hydrogen occupation sites. Additional Ti–C bonds from chemical bonding of Ti with carbon, which occupies octahedral interstitials, appears in TiH_2 due to intimate contact between graphite and TiH_2 nanoparticles embedded into an amorphous graphite matrix. Mixed configurations around Ti atoms with proportional combination of local Ti–H and Ti–C bonds significantly decrease the thermal stability of TiH_2.

Keywords: TiH_2; Graphite; Ball milling; Temperature-programmed desorption; X-ray emission and absorption spectroscopy; TEM; Local bonding structure

1. Introduction

Transition metals are known to accommodate a great amount of hydrogen and have been studied as promising materials for hydrogen storage [1]. The development in metal-hydride technology required a detailed study of hydrogen interaction with metals and alloys. Much work has been performed on titanium hydride, as a model system, because it possesses one of the highest absorptive capacities among the metal-hydrides [2]. High-energy ball milling of Ti in H_2 atmosphere has been shown to be a simple, low-cost and highly effective technique to synthesize titanium hydride nanocrystalline powders at room temperature [3] by crashing the surface titanium oxide and making the fresh titanium surface accessible for interaction with H_2. It is found that mechanical treatment of metal-hydrides greatly improves the hydrogen absorption–desorption kinetics [4], and that the addition of carbon-containing compounds or graphite to metal powders before milling improves the metal-to-hydrogen reactivity [5]. The mechanism of the stimulating effect of graphite addition is not studied in detail, in spite of its importance for efficient synthesis of hydrogen storage materials. In the present work we have studied the local atomic and electronic structure of Ti atoms in mechanically activated TiH_2 and TiH_2/graphite mixtures with the help of temperature-programmed desorption (TPD) and X-ray emission and absorption spectroscopy.

2. Experimental

2.1. Preparation procedure

TiH_2 powder (99% pure, 325 mesh from Aldrich) or mixtures of TiH_2 powder and pyrolytic graphite (99% pure, $S = 3\,m^2/g$) were milled in He flow for 30, 62 and 126 min

* Corresponding author.
E-mail address: om@polymer.chph.ras.ru (O. Morozova).

0925-8388/$ – see front matter © 2004 Elsevier B.V. All rights reserved.
doi:10.1016/j.jallcom.2004.11.031

using a flow mechanochemical reactor (average energy intensity of 1.0 kW/kg) at room temperature and atmospheric pressure. A stainless steel container was loaded with 1.8 g of TiH_2 or TiH_2/graphite reaction mixture (1.5 g TiH_2 + 0.3 g graphite) together with 19.8 g of hardened steel balls (3–5 mm diameter). The reactor input was connected to a setup for gas mixture preparation; the outlet was combined on-line with a gas chromatograph to monitor the effluent gas composition. A flow rate of 8–10 ml/min was used. The effluent gas was analyzed every 5–10 min in order to study dynamics of hydrogen evolution from TiH_2 during milling. After each run, the sample was passivated in helium flow for 2–3 h before taking it out on atmosphere for further investigations. The specific surface area *S* of original and as-milled powders was measured by low-temperature Ar adsorption.

2.2. Temperature-programmed desorption (TPD)

The TPD measurements were carried out at a heating rate of 10 K/min from 290 to 940 K under flow conditions (Ar, flow rate of 100 ml/min). A flow quartz reactor was charged with a 0.1-g sample of testing powder. The testing powder was mixed with quartz powder (∼70 wt.%) in order to minimize the temperature difference between the sample and surroundings of the reactor caused by the heat of hydrogenation/dehydrogenation reaction and to prevent the powder from caking. The reactor with a sample was blown through with Ar before heating. After the hydrogen desorption the sample was quickly (during ∼10–15 min) cooled to room temperature in Ar flow. H_2 emission was monitored continuously with a PC interfaced to a gas chromatograph with a thermal-conductivity detector. The amount of hydrogen emitted was calculated on the base of special calibration through integrating the area under the TPD curve. TPD was accompanied by XRD powder analysis.

2.3. Transmission electron microscopy (TEM)

The TEM and HRTEM measurements were carried out on a Philips EM 420 ST electron microscope with a resolution limit of 0.3 nm and an accelerating potential of 120 kV. The TEM samples were prepared in an ethanol suspension and placed on copper grids covered by a network of amorphous carbon, which permits to distinguish between carbon from the grid and carbon from the sample.

2.4. Soft X-ray fluorescence measurements

X-ray fluorescence measurements were performed at undulator beamline BL27SU at Spring-8 using soft X-ray fluorescence endstation. A well-focused beam, less than 10 μm in vertical direction, allowed to use a slitless spectrometer, which improved a throughput of instrument and detection efficiency. A slitless spectrometer with a spherical VLS (Varied Line Spacing) grating and back-illuminated (BI) charge coupled device (CCD) detector [6] provided an energy resolution of $E/\Delta E = 1000$.

3. Results and discussion

3.1. Kinetics of TiH_2 decomposition under mechanical treatment

Partial decomposition of TiH_2 was induced by mechanical treatment in He flow. The parameters of this process are listed in Table 1. The original TiH_2 powder lost about 5 mol% of H_2 during 60 min of milling (Fig. 1a). After the milling, the specific surface area of the sample increased from 0.32 to 6 m^2/g. Significant broadening of XRD peaks was also observed. The microblock size estimated from XRD patterns is ∼130 Å. Computer fitting of this pattern (quantitative phase analysis) [7] points to a two-phase composition containing ∼60% of $TiH_{1.94}$ cubic ($a = 0.445$ nm, JCPDS 25-982) and ∼40% of TiH_2 tetragonal ($a = 0.319$ nm, $c = 0.435$ nm) phases.

The H_2 evolution from TiH_2/graphite powder was accompanied by formation of CH_4 and C_2H_6 after a short induction period (Fig. 1b). As was shown previously [8], hydrocarbon formation is indicative to close intermixing of hydride and graphite. After 62 and 126 min of milling, TiH_2/graphite

Table 1
Conditions and results of mechanical activation

Sample	Treatment conditions	Phase composition	S (m^2/g)	H_2 evolution (mol/g TiH_2)	Graphite consumption (at.%)
1	TiH_2 as-received	TiH_2 tetragonal ($a = 0.447$ nm; $c = 0.440$ nm; $c/a = 0.98$)	0.32		
2	TiH_2 (1.8 g); He flow; 60 min	$TiH_{1.9}$ cubic ($a = 0.445$ nm); TiH_2 tetragonal ($a = 0.319$ nm; c = 0.435 nm; $c/a = 1.36$)	6	1×10^{-3} (5 mol%)	
3	TiH_2 (1.5 g) + graphite (0.3 g); He flow; 30 min	Graphite, $TiH_{1.9}$ cubic (a = 0.445 nm); TiH_2 tetragonal ($a = 0.317$ nm; $c = 0.438$ nm; $c/a = 1.38$)	48		
4	TiH_2 (1.5 g) + graphite (0.3 g); He flow; 62 min	Graphite, TiH_2 cubic ($a = 0.445$ nm)	38.2	1.2×10^{-3} (∼6 mol%)	∼0.3
5	TiH_2 (1.5 g) + graphite (0.3 g); He flow; 126 min	Graphite, TiH_2 cubic ($a = 0.445$ nm)	52.4	1.05×10^{-3} TiH_2 (∼5.2 mol%)	2.7

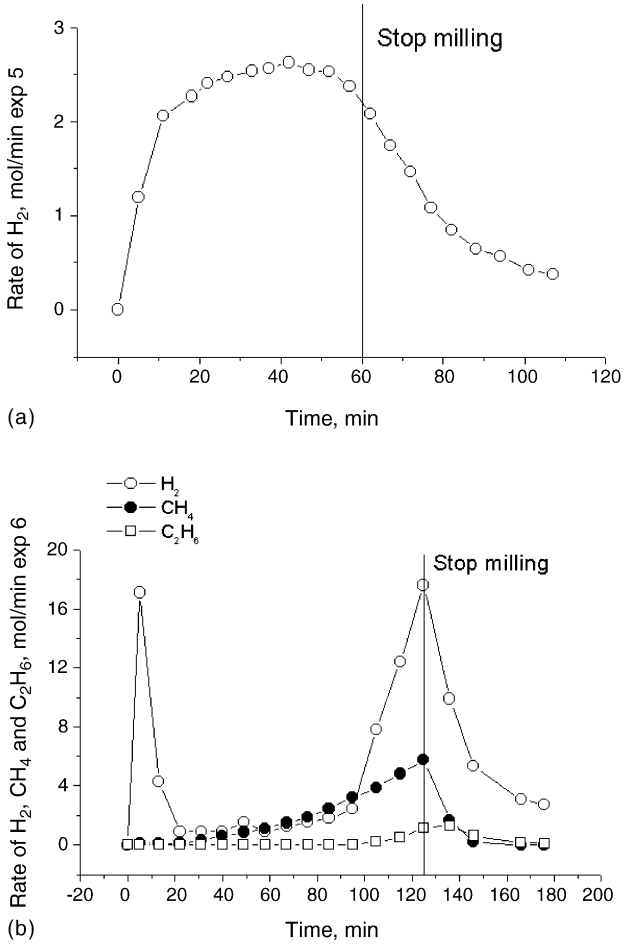

Fig. 1. Kinetics of H_2 evolution induced by mechanical treatment of (a) TiH_2 and (b) TiH_2/graphite mixture.

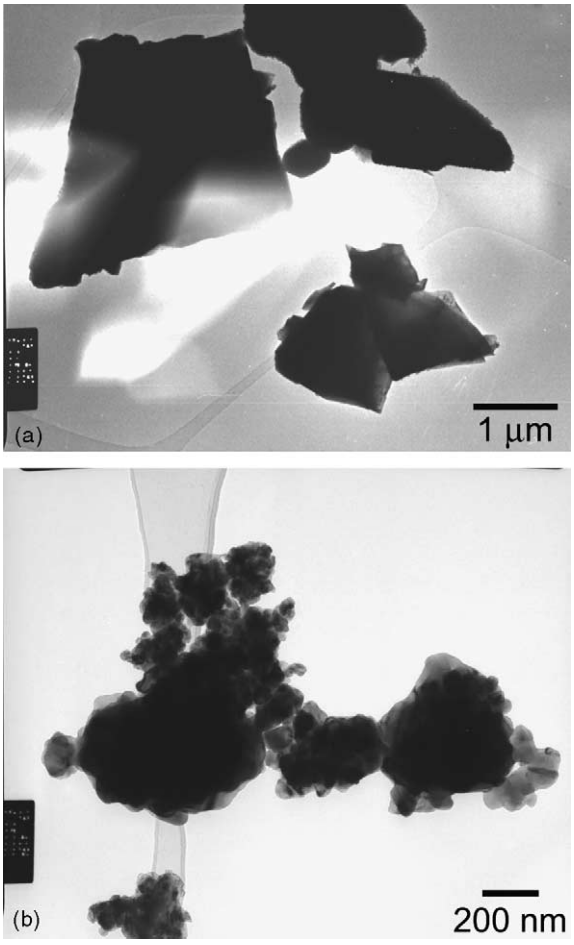

Fig. 2. (a) TEM micrograph of the original TiH_2 powder. (b) TEM micrograph of TiH_2 powder milled for 60 min.

samples lost ∼6 mol% of H_2 (in the form of H_2 and hydrocarbons). The rather low hydrogen loss after 126 min of milling may be explained by significant re-adsorption of H_2 on the active surface of graphite mechanically activated resulting in the formation of partially hydrogenated graphite: high concentrations of surface CH_2- and CH_3- groups were detected by FTIR. The specific surface area of the samples after 30, 62, and 126 min of milling was measured as 48, 38.2, and 52.4 m^2/g, respectively, because of the extremely large specific surface area of graphite, which increased from 3 to ∼190–280 m^2/g. XRD patterns demonstrate very broad titanium dihydride peaks. No peaks could be attributed to Ti–C or Ti–C–H phases. Only a weak increase in the background was observed after 126 min of milling. The average microblock size of these samples was estimated as 130 and 104 Å, respectively. Close analysis of XRD patterns gave poor information.

3.2. Microstructure and morphology of as-milled powders

According to TEM data rather large original TiH_2 particles (Fig. 2a) are under the mechanical treatment transformed to loose particles consisting of thin scales or flakes agglomerated together (Fig. 2b), where the individual particles reach sizes of some tens of nm. Strong surface strain contrast being observed on the particle surface is indicative to the high concentration of strains.

The picture is completely different for samples milled together with graphite, the latter playing an outstanding role in this process. The original graphite consists of compact crystalline particles. After 30 min of milling, see Fig. 3, it has disintegrated to loose bands, tubes and flakes, which are partly crystalline and partly amorphous. This carbon now wraps up the hydride particles, which themselves are nanosized. After 126 min of milling, the carbon is almost completely amorphous, and forms a sponge-like structure with hydride particles embedded in the cavities, see Fig. 4. These hydride particles consist of thin flakes, which appear dark in the micrograph.

3.3. H_2 desorption from original and as-milled TiH_2 samples

The TPD parameters are listed in Table 2. The TPD spectrum of original TiH_2 powder consists of a rather nar-

Fig. 3. TEM micrograph of TiH_2/graphite mixture milled for 30 min.

Table 2
TPD parameters of original and as-milled TiH_2 powders

Sample	H_2 evolution (mol/g TiH_2)	T (K_{max})	E_a (kJ/mol)*	E_a for beginning of desorption (kJ/mol)*
1	1.78×10^{-2}			
	1.53×10^{-3}	747		210 ± 7.8
	1.63×10^{-2}	817	192.4 ± 6.3	
2	1.8×10^{-2}			
		633		27 ± 0.7
		796	161 ± 5.7	
3	$\sim 1.9 \times 10^{-2}$			
	3.3×10^{-3}	629		37.9 ± 1.4
	5.5×10^{-3}	705		
	1×10^{-2}	800	197 ± 7.4	
4	$\sim 1.7 \times 10^{-2}$			
	4.1×10^{-3}	608		35.7 ± 0.5
	7.6×10^{-3}	686	209 ± 8.7	
	4.6×10^{-3}	775		
5	1.68×10^{-2}			
	2.5×10^{-3}	607		39.7
	9.2×10^{-3}	674		
	5.1×10^{-3}	773	183 ± 6.5	

* Ea is calculated in suggestion that the H_2 evolution rate is proportional to hydrogen concentration in the sample. Linear fits of TPD curves were constructed as $\ln W/C^2 - 1/T$ (K) plots. It points to an effective second order process (surface recombination of H atoms seems to be a rate-determining step).

Fig. 4. TEM micrograph of TiH_2/graphite mixture milled for 126 min.

row (of ∼80° half-width) single peak with a small low-temperature shoulder (Fig. 5a) which is indicative to uniform (or rather narrow) type of hydrogen occupation centers in the TiH_2 lattice. A small low-temperature shoulder may be attributed to H atoms being localized in intergranular positions.

TPD spectrum of the as-milled TiH_2 powder (Fig. 5b) consists of one very broad peak or a number of overlapping peaks, the parameters of which are different from those of the TPD peak recorded for the original sample. As follows from Lorentzian fitting of the TPD curve, the half-width of the highest-temperature peak increased up to 110°. It indicates a very broad but more or less uniform distribution of hydrogen occupation centers. There is no specific discrete type of positions for H atom localization except for the first low-temperature peak, for which specific surface states (strains) may be responsible. The concentration of this type of sites is rather low.

Very similar TPD spectra were observed for all of the as-milled TiH_2/graphite powders: two-peak curves consisting of broad low-temperature peak and rather narrow high-temperature peak (see Fig. 6a–c). According to Lorentzian fitting, the low-temperature peak consists of two completely overlapping peaks. The high-temperature peak half-width and other TPD parameters are very similar to these measured for TPD peak of original TiH_2. This fact allows us to attribute the high-temperature peaks observed in the aforementioned TPD spectra to the decomposition of TiH_2 in the

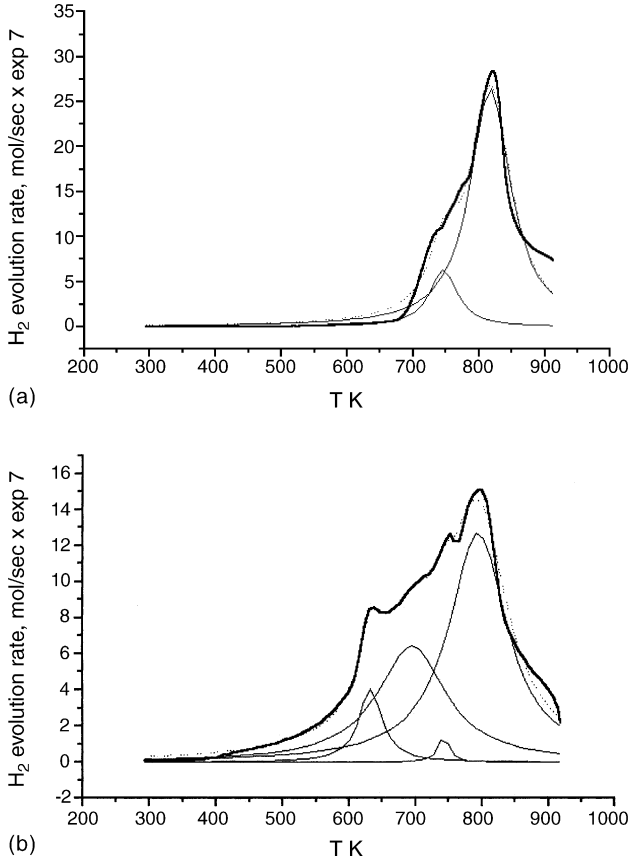

Fig. 5. TPD spectra for (a) TiH_2 original and (b) as-milled TiH_2.

original state. That means that even after 126 min of mechanical treatment with graphite, some part of hydrogen occupation centers (down to 25–30 mol%) are similar to those in the original TiH_2. The major part of H atom positions (low-temperature peaks) may be attributed to the positions in TiH_2 lattice modified by carbon atoms. This suggestion follows primarily from the morphological features of as-milled powders and from the following experimental facts: (1) CH_4 formation and (2) formation of cubic Ti_2C phase (up to 18 mol%) after TPD procedure. The first is indicative to the formation of so-called "active" carbon—interstitial carbon atoms in hydride lattice (see, for example [9]). This kind of carbon is active enough to react with H atoms to give methane. The second demonstrates that during the heating interstitial C atoms diffuse into the bulk to form Ti_2C phase. Thus, in the case of TiH_2/graphite powder, two discrete types of hydrogen occupation sites are present. First, in regular TiH_2 lattice. Second, near interstitial carbon atoms.

Based on the TEM and TPD measurements one can conclude that the mechanical treatment of TiH_2 and TiH_2/graphite powders results in the formation of a high concentration of structural defects in the surface and in the bulk of the samples.

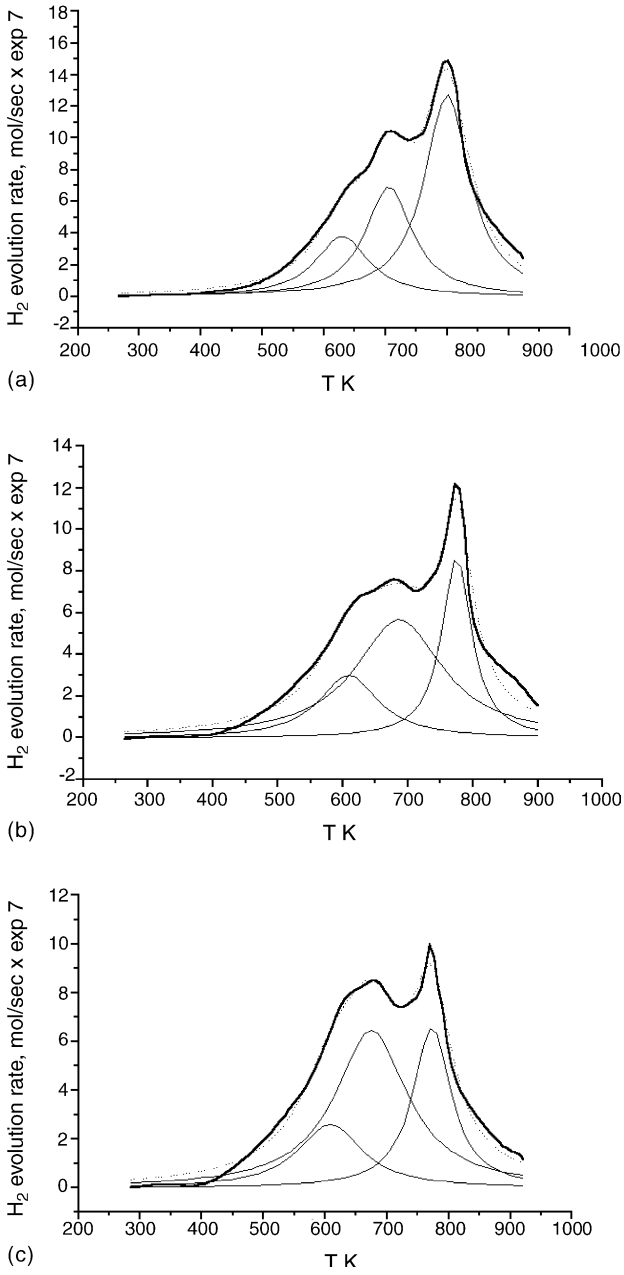

Fig. 6. TPD spectra for (a) 30-min milled, (b) 62-min milled, and (c) 126-min milled TiH_2/graphite powders.

3.4. Local atomic and electronic structure of Ti atoms

We have measured Ti L-X-ray emission (XES) spectra, which probe Ti 3d occupied valence states, respectively. Fig. 7 shows Ti L_l ($3s \rightarrow 2p_{3/2}$ transition), Ti Lα ($3d4s \rightarrow 2p_{3/2}$ transition) and Ti Lβ ($3d4s \rightarrow 2p_{1/2}$ transition) emission spectra. Ti Lα and Ti Lβ XES are normalized to the intensity of Ti L_l XES, which does not participate in the chemical bonding. The fine structure of Ti Lα XES in TiH_2 is found to be quite different with respect to that of pure Ti (Fig. 8). A significant change is observed in Ti Lα XES: an additional low-energy subband (B) located at

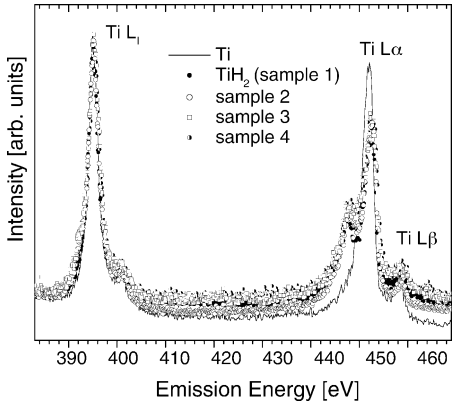

Fig. 7. Ti L_l, Ti Lα and Ti Lβ XES of Ti, TiH_2 and TiH_2/graphite mixtures after ball milling.

~447.8 eV, i.e., about 4.6 eV lower than the most intensive line (A) appeared. According to electronic structure calculations of TiH_2 [10,11], this subband is formed by Ti3d-H1s bonding. Therefore, we ascribe an additional subband *B* to a hydrogen-induced state of Ti. The mechanical treatment of TiH_2 will not induce noticeable changes in XES of titanium dihydride except some broadening of peak B, which can be due to some structural defects. On the other hand, ball milling of TiH_2 with graphite leads to the appearance of an additional subband C located between A and B subbands (Fig. 9a). The energy position of subband C is found to be very close to Ti Lα XES of TiC [11] indicating for appearance of Ti–C bond in the mechanically activated TiH_2/graphite mixture.

According to XRD measurements, two-phase composition containing ~60% of $TiH_{1.94}$ cubic and ~40% of tetragonal phases is observed for sample 2. However, the band structure calculations show [10,11] that Ti 3d density of states (DOS) of tetragonally distorted TiH_2 (for $c/a = 0.926$ and 1.068) is very similar to that for the cubic compound with CaF_2 structure where H atoms occupy tetrahedral interstices in the fcc metal lattice. The differences are found only in the close vicinity of the Fermi level caused by the splitting of bands in this energy region. However, these differences are

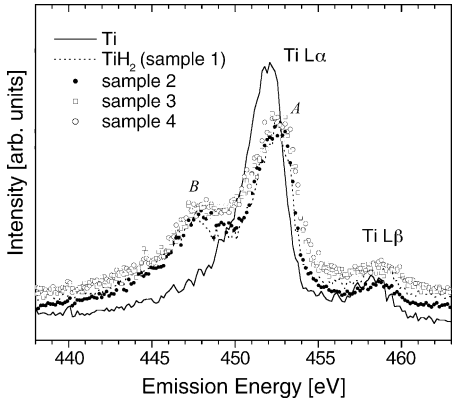

Fig. 8. Ti Lα and Ti Lβ XES of Ti, TiH_2, mechanically activated TiH_2 and TiH_2/graphite mixtures.

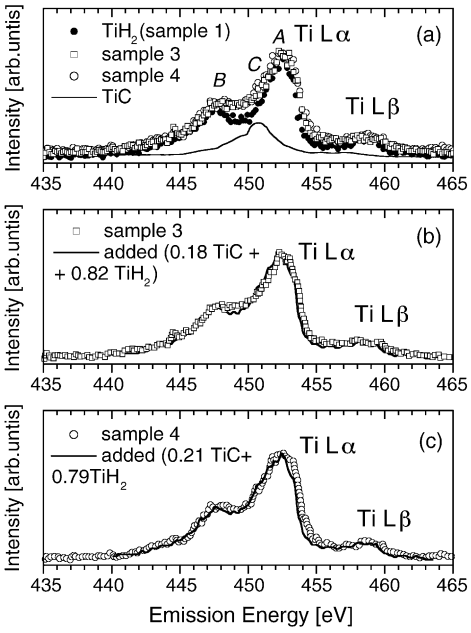

Fig. 9. (a) Comparison of TiLα and Ti Lβ XES of mechanically activated TiH_2/graphite mixtures with spectra of reference samples TiH_2 and TiC. (b and c) Simulation of TiLα and Ti Lβ XES of mechanically activated TiH_2/graphite mixtures by superposition of spectra of untreated TiH_2 and TiC.

not seen in Ti Lα XES because of limited energy resolution. This means that Ti Lα XES is not sensitive to tetragonal distortion and, therefore, can not be used to distinguish hydrogen occupation for tetragonal and cubic dihydride phases.

A broadening of Ti Lα XES for mechanically activated TiH_2/graphite mixture can be due to the contribution of additional Ti–C bonds from chemical bonding of Ti atoms with carbon atoms which occupy octahedral interstitials. The energy position of Ti Lα XES of TiC located between A and B maxima of TiH_2 (Fig. 9a) directly indicates for this conclusion. Superposition of Ti Lα XES of TiH_2 and TiC reproduces spectra of mechanically activated TiH_2/graphite mixture quite well (see Fig. 9b and c. Therefore, a structural state of mechanically activated TiH_2/graphite mixture can be characterized by mixed configurations around Ti atom with proportional combination of local Ti–H and Ti–C bonds indicative of occupation of tetrahedral and octahedral interstitials by hydrogen and carbon atoms, respectively. Using XES data, we can estimate the content of C atoms introduced in TiH_2 lattice around 18–21 at.%, which is in a good agreement with 13, 16 and 18 at.% in the samples 3, 4 and 5, respectively, obtained through the quantitative analysis of XRD patterns measured after TPD. From these results follows that about 18 at.% of interstitial C atoms change the Ti–H binding energy for 70–95 at.% of H atoms in TiH_2 lattice.

4. Conclusions

In conclusion, our results show that the addition of graphite TiH_2 powder under mechanical activation moves

hydrogen desorption, as measured by TPD, to lower temperatures, as compared to the pure powder, milled or unmilled. Even for pure powder, milling already leads to a noticeable decrease in desorption temperature, but the addition of graphite triggers a further decrease of about 150 °C altogether. Moreover, an additional desorption peak appears in the presence of graphite. In addition, the kinetics of hydrogen evolution is greatly accelerated by the addition of graphite. The corresponding microstructures show that milling of the pure hydride leads to a drastic fragmentation of the powder particles, accompanied by the introduction of a high defect density. When graphite is added, the hydride is still fragmented, and the graphite turns into entangled and coiled ribbons, which are partly crystalline and partly amorphous and wrap up the hydride fragments. After further milling, the graphite forms a completely amorphous sponge-like structure, in which the now only some nm large hydride particles are embedded. Along with this, XRD reveals that the hydride transforms from tetragonal TiH_2 to cubic $TiH_{1.9}$, an occurrence that is completed after 62 min of milling the TiH_2/graphite mixture, but completed only to about 60% after 60 min of milling the TiH_2 alone. The evolution of CH_4 and C_2H_6 during milling was observed. XES reveals a TiC peak indicating a combination of Ti–H and around 18–20% Ti–C bonds, where H occupies tetrahedral, and C octahedral interstitial sites.

The enthalpy of formation of TiC is 92 kJ/g-atom that of TiH_2 is 48 kJ/g-atom [12]. So, when carbon atoms diffuse into the hydride lattice, local Ti tends to form Ti–C bonds, driving out H atoms in the vicinity, which then forms methane or ethane evolving at the surface. It can be assumed that this occurs in near-surface-sites of the hydride, leaving enough of the observed Ti–H bonds to show the high-temperature TPD peak indicative of undisturbed TiH_2.

To summarize, the addition of graphite to TiH_2 is a promising method to enhance hydrogen evolution kinetics and lower the evolution temperature during ball milling of the hydride, since carbon has a greater affinity to titanium than hydrogen.

Acknowledgements

This work is supported by the Research Council of the President of the Russian Federation (Grant NSH-1026.2003.2) and the Russian Science Foundation for Fundamental Research (Project 04-03-32215).

References

[1] K.M. MacKay, Hydrogen Compounds of the Metallic Elements, Spon, London, 1965.
[2] G. Alefeld, J. Volkl, Hydrogen in Metals, Springer-Verlag, Berlin, 1978.
[3] J.-L. Bobet, C. Even, J.-M. Quinesset, J. Alloys Compd. 348 (2003) 247.
[4] A. Zaluska, L. Zaluski, J.O. Ström-Olsen, J. Alloys Compd. 288 (1999) 217.
[5] S. Bouaricha, J.P. Dodelet, D. Guay, J. Huot, R. Shulz, J. Alloys Compd. 325 (2001) 245.
[6] T. Tokushima, Ph.D. Thesis, Hiroshima University, 2003.
[7] E.V. Shelekhov, T.A. Sviridova, Met. Sci. Heat Treat. 42 (2000) 309.
[8] Ch. Borchers, A.V. Leonov, O.S. Morozova, J. Phys. Chem. B 106 (2002) 1843.
[9] J.G. Mc Carty, H. Wise, J. Catal. 57 (1979) 406.
[10] W. Wolf, P. Herzig, J. Phys. Condens. Matter 12 (2000) 4535.
[11] D.W. Fischer, J. Appl. Phys. 41 (1970) 3561.
[12] O. Knacke, O. Kubaschewski, K. Hesselmann (Eds.), Thermochemical Properties of Inorganic Substances, Springer, Berlin, 1991.